Journal of Earth Science, *Vol. 23*, *No. 5*, *p. 731–743*, *October 2012* *ISSN 1674-487X*
Printed in China
DOI: 10.1007/s12583-012-0280-3

Deepwater Canyons Reworked by Bottom Currents: Sedimentary Evolution and Genetic Model

Caili Lü (吕彩丽)
Key Laboratory of Marine Geology & Environment, *Institute of Oceanology*, *Chinese Academy of Sciences*, *Qingdao* 266071, *China*; *Graduate University of Chinese Academy of Sciences*, *Beijing* 100049, *China*
Yongjian Yao* (姚永坚), **Yuehua Gong** (龚月华)
Guangzhou Marine Geological Survey, *Guangzhou* 510075, *China*
Shiguo Wu (吴时国)
Key Laboratory of Marine Geology & Environment, *Institute of Oceanology*, *Chinese Academy of Sciences*, *Qingdao* 266071, *China*
Xuejie Li (李学杰)
Guangzhou Marine Geological Survey, *Guangzhou* 510075, *China*

ABSTRACT: Based on multi-beam bathymetric data and 2D high-resolution, multi-channel seismic profiles, combing ODP1148 drilling data, the morphology, internal sedimentary architecture, and evolution pattern of 17 deepwater canyons from the Middle Miocene to present are documented in the northern Baiyun (白云) sag (BS), Pearl River Mouth basin (PRMB), and northern South China Sea (SCS). There exist six seismic architectural elements in these canyons, including basal erosive surfaces (BES), thalweg deposits (TD), lateral migration packages (LMP), mass transport deposits (MTD), canyon margin deposits (CMD), and drape deposits (DD). According to the stratigraphical ages and geometrical features of these canyons, their formation and evolution processes are divided into three stages: (1) Middle Miocene scouring-filling, (2) Late Miocene lateral migration, and (3) Pliocene–Quaternary vertical overlay. An auto-cyclic progressive process of eroding and filling by turbidity currents results in the scouring-filling and vertical overlay; bottom currents are responsible for the remarkable asymmetry between the two flanks of canyons; and faults are inherent dynamic forces triggering these can yons. It is inferred that these canyons are caused by the double effects of turbidity and bottom currents under the control of faults as inherent dynamic forces.

KEY WORDS: deepwater canyon-channel, bottom current, turbidity current, lateral migration, South China Sea.

This study was jointly supported by the CAS Knowledge Innovation Program of China (No. KZCX2-YW-229), and the National Natural Science Foundation of China (Nos. 40930845, 2009CB219505).
*Corresponding author: yjyao64@yahoo.com.cn

Manuscript received April 2, 2011.
Manuscript accepted September 15, 2011.

In the 1940s, the deepwater canyon-channel system was found on the passive continental margin of

North America for the first time. Since then, it has been one of the key focuses in the petroleum industry (Heinio and Davies, 2007). Channel-levees, as one of parts of deepwater canyon-channel system, can act not only as good hydrocarbon reservoirs but also as important paths transporting terraneous components from lands to deep-sea basins, playing a role of classification and constraint to sediments. Deepwater canyon-channels developed mainly in the slope of continental margins. We study their genetic mechanisms and evolutions, not only consisting in finding deepwater hydrocarbon reservoirs and helping to establish their geological theories but also speculating the sedimentary sources of deep-sea basins according to their evolution characteristics, restoring their specific paleogeographic environments of these basins, and exploring the dynamic evolution mechanisms of continental margins.

Most modern deepwater canyon-channels in the world have been documented from large passive-margin fans, supplied by major rivers carrying huge volumes of dominantly fine-grained sediments (Wynn et al., 2007), e.g., Amazon (Damuth and Flood, 1985), Mississippi (Bouma et al., 1984), Zaire (Droz et al., 1996), Bengal (Emmel and Curray, 1985), Indus (Kolla and Coumes, 1987), and Rhone and Nile Fans (Wynn et al., 2007). This paper regards the deepwater canyons in Baiyun sag (BS) in the northern continental slope of South China Sea (SCS) as the research subject, which develop in the slope environment of marginal sea basin and has the unique characteristics of formation and sedimentary evolution processes. These are of great significance to explore their genetic mechanisms and sedimentary models, demonstrating the paleogeographic environments where they exist and improving the genetic theories of deepwater canyon-channels. Based on the multi-beam bathymetric data and 2D high-resolution, multi-channel seismic profiles, this study reveals the sedimentary characteristics of deepwater canyons. Also, referring to the lithological and paleoenvironmental information that is provided by the ODP1148 drilling and those oil boreholes located in BS and the shelf break, and combing biostratigraphy and sequence stratigraphy and regional comparative methods, this paper comprehensively analyzes and explores the formation and sedimentary evolution processes of deepwater canyons.

GEOLOGICAL SETTING

The BS, which is located in the Zhu II depression, Pearl River Mouth basin (PRMB), northern SCS, whose shape is like a butterfly, is nearly W-E strike and covers an area of more than 20 000 km^2 that is about 200–2 000 m water depth (WD). The northern side is Panyu low relief; the west is bordered on the magmatic active zone and fundamental fractures, which strike in the NW, and is contiguous with Shenhu uplift and the western section of Zhu II depression; the east is Dongsha uplift (Dong et al., 2008) (Fig. 1). The BS, a semi-closed slope basin, is the most representative deepwater continental slope sedimentary province in the northern SCS. This province encountered compressing during the Mesozoic era, rifting and subduction along the Manila trench during the early and late of Cenozoic era, respectively, which make its basement become more complicated (Xie et al., 2006; Huang et al., 2005). On both western and eastern sides of BS, the shelf break is gentle, but the shelf break in the north is very steep where several deepwater canyons deeply cutting the stratum occur. Since the Late Oligocene and the seafloor spreading of SCS, BS has existed in deepwater environments; after the Miocene, the whole BS enters into bathyal environments (Zhao, 2005).

SEDIMENTARY CHARACTERISTICS OF DEEPWATER CANYONS

Topography Features

In the northern slope of BS, there occurs complicate submarine canyon-channel system, which develops below the shelf break and about 200 m WD. In the 3D topography map made by multi-beam sounding (Fig. 2), there are at least 21 canyons to be identified and four small ones of which in the west are located in the source of the Zhujiangkouwai Submarine Grand Canyon. However, it is very difficult to identify the four small canyons in the 2D seismic profiles (Fig. 3), which may be due to their too small size or too shallow erosion and should be gully in the grand canyon rather than canyons formed by the long-term eroding and filling of flows. Therefore, there are only 17 deepwater canyons numbered C1–C17 from west to east, located on the east of Zhujiangkouwai submarine grand canyon in the northern slope of BS, to be chosen as research subjects in this work (Figs. 2 and 3). All 17 canyons, showing linear-like characteristics, arranging in sub-parallel each other and extending in near N-S direction, are approximately oblique with the slope. In the downstream or near the end of canyons, there are abrupt changes from the south to the southeast in their strike directions, and some of them even turn to the near W-E direction. The canyons begin to originate below the shelf break and terminate at about 1 500 m WD in the northern slope of BS, and their main parts are at about 500–1 500 m WD (Fig. 2). It is concave in the axes of canyons whose thalweg morphology changes with the gradient, and especially C2 and C3 that show the most obvious characteristics.

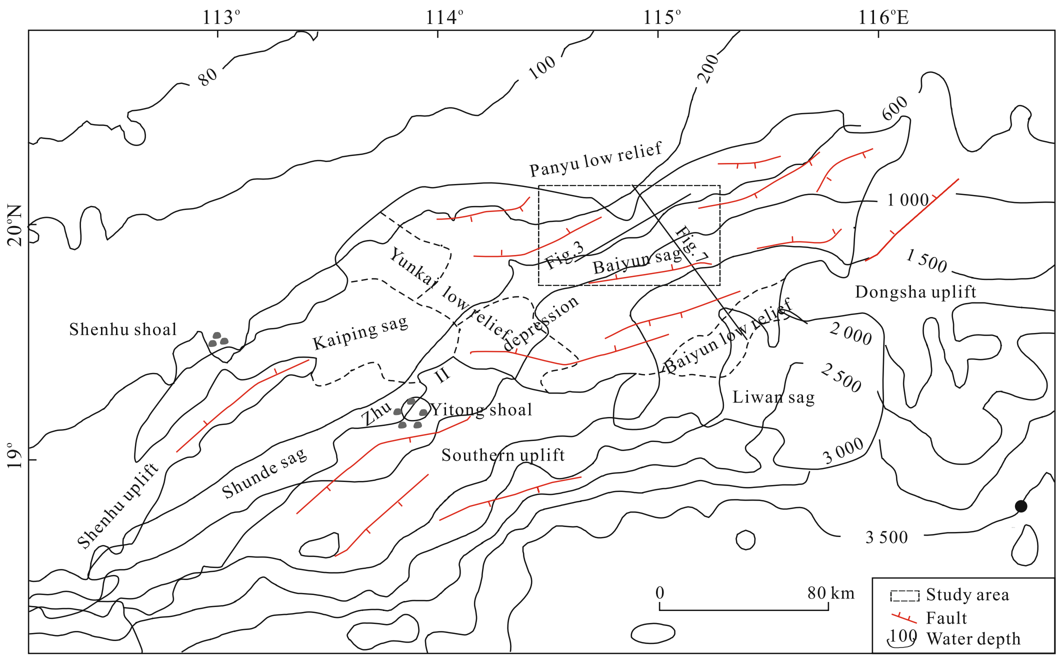

Figure 1. Sketch map showing the location of the study area (dashed line box) and structural units in the northern SCS.

Yu and Chang (2009) have pointed out that a submarine canyon-channel developing in continental margins is still in its immature stage when it has not deeply eroded into the continental shelf. In contrast, a submarine canyon-channel eroding into the continental shelf can receive a lot of sediments from lands and strengthen its headward erosion into lands, making it further incise deeply and gradually reaches to its mature stage. The deepwater canyons in the study area have not eroded into the shelf and are not connected with rivers on the land receiving relatively few sediments and possessing weaker headward erosion (Fig. 2). Thus, these deepwater canyons are in an immature stage, but they become more mature in the west than in the east.

Interestingly, these 17 deepwater canyons in the study area show similar characteristics in the plane, but they can be divided into three groups according to the WD and the distance between their headwaters to the shelf break (Fig. 2). The first group begins to originate in the near shelf break at about 250 m WD, including C1–C3; the headwaters of the second group are farther away from the shelf at about 500 m WD, including C4–C9; and the third group are the farthest away from the shelf at about 900 m WD, including C10–C17.

Deepwater canyons C2–C3, originating in the vicinity of shelf break and ending at about 1 000 m WD, are straighter than other ones. As shown in the 2D high-resolution multi-channel reflection cross-section seismic profiles (Fig. 4), the flanks of canyons in the upper are steep and have a small aspect ratio (width/depth) showing V-type, which are dominated by eroding, while their flanks in the lower are gentle and have a large aspect ratio showing U-type, which are dominated by both eroding and sedimentation. They are similar with the typical turbidity canyon-channel—Amazon canyon-channels, which are most deeply researched in the world so far. In the cross-section, the Amazon canyon-channels show V-type in the upper and U-type in the lower, which are mainly due to the long-term eroding-filling of turbidity currents down the slope (Pirmez and Imran, 2003).

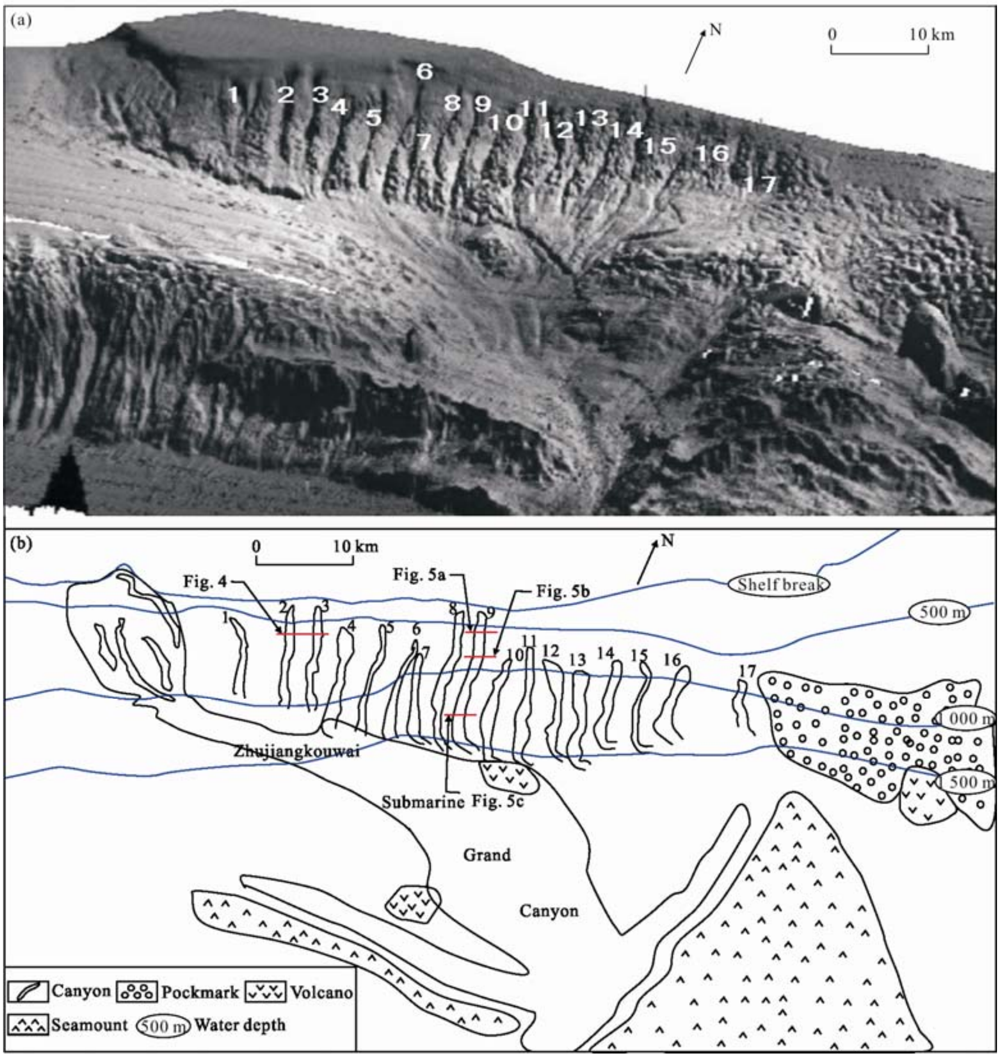

Figure 2. Topography map of the 17 deepwater canyons in the study area. (a) 3D multi-beam bathymetric topography map; (b) the drawing line.

Kolla et al. (2007) have suggested that there is only one distributary canyon-channel to be active in the same deepwater canyon-channel-levee system during a specified period. However, in the study area, all 17 deepwater canyons are very close to each other and show characteristics of migrating towards the northeast at the same time; then, it suggests that they are almost active simultaneously, so their genetic mechanism may vary from the typical deepwater turbidity canyon-channels in the world.

Seismic Responses of Deepwater Canyons

There are four stratigraphic boundaries to be identified in the 2D high-resolution multi-channel

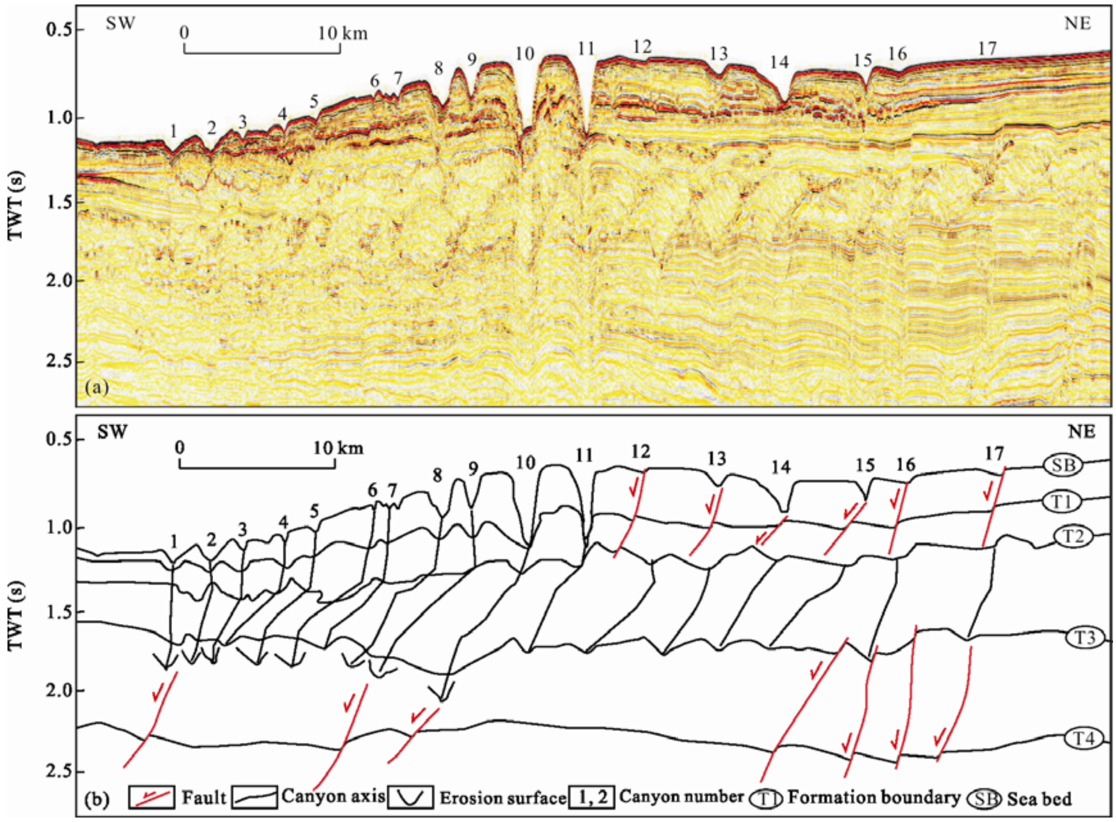

Figure 3. Cross-section profile of canyons in the study area (the seismic line is shown in Fig. 1). (a) Original seismic section; (b) the drawing line.

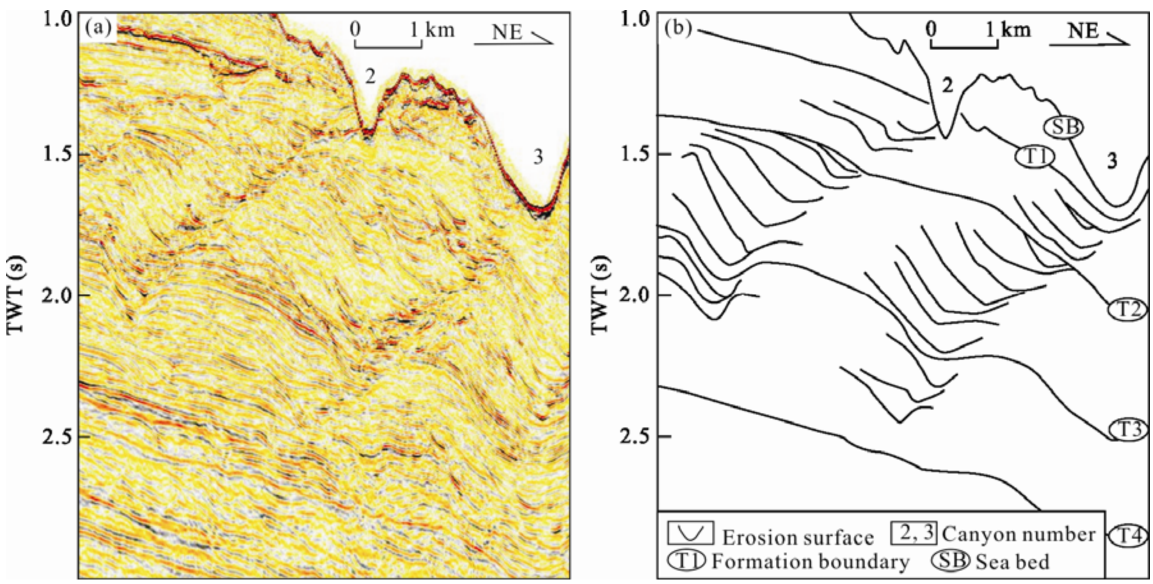

Figure 4. Cross-section seismic reflection profiles through C2–C3 (the measuring line is shown in Fig. 2). (a) Original seismic profile; (b) the drawing line.

seismic profiles, including T1 (Quaternary/Pliocene), T2 (Pliocene/Upper Miocene), T3 (Upper Miocene/Middle Miocene), and T4 (Middle Miocene/Lower Miocene) (Table 1), and the canyons in the study area are developed in the Middle Miocene (after T4) (Fig. 3). All studied canyons show similar genetic characteristics and evolution processes, which include their bottom cross-section appearing as V-type, their axes migrating consistently to the northeast and the vertical overlay and filling characteristics. In their extending direction and the adjacent canyons at the same WD, seismic structural units show basically the same shapes and overlay patterns, that is, a single canyon changes gradually from lateral migration to the northeastern direction in the proximal upper slope to vertical overlay in the distal lower slope. Canyon C9, which is located in the center of the study area and in the middle stage of developing processes, can be representative of all studied 17 canyons. Then, canyon C9 is chosen to explore further as shown in Fig. 2.

Based on seismic facies characteristic parameters (including external morphology, internal reflection texture, amplitude, and continuity) and seismic reflection termination, the seismic reflection units of deepwater canyons are divided into 10 classes (Zhu et al., 2010; Weimer and Slatt, 2007), including basal erosive surfaces (BES), thalweg deposits (TD), lateral migration packages (LMP), mass transport deposits (MTD), outer levee-overbank deposits (OL-OD), inner levee deposits (ILD), canyon margin deposits (CMD), drape deposits (DD), canyon-channel-lobe zones (CLZ), and lobe/sheet sandstone deposits (L/SSD), and their specific characteristics are shown in Table 2. The deepwater canyons in the study area are mainly made up of six seismic reflection units, including BES, TD, LMP, MTD, CMD, and DD. After analyzing their seismic facies, sedimentary facies, and lithofacies using the method by Prather et al. (1998), we find that fine-grained components mainly containing clays and silts are up to approximately 95%, which is concordant with the percentage of fine-grained sediments (mainly being silts) transported by turbidity currents (Pirmez et al., 2000).

In the cross-section A (Fig. 5a), there are at least two normal faults dipping to the southwest under the bottom of canyons, and the two flanks on either side of a single canyon are both steep showing V-type and high relief. It shows characteristics of vertical overlay between the two single adjacent canyons, and there is a small amount of deposition in the thalweg of can-

Table 1 Stratigraphic division in the northern slope of BS

Chronostratigraphic unit		Symbol	Stratigraphical ages (Ma)	Seismic reflection boundary
Quaternary		Q		
			1.8	T1
Pliocene		N_2		
			5.3	T2
Miocene	Upper Miocene	N_1^3		
			10.5	T3
	Middle Miocene	N_1^2		
			16.5	T4
	Lower Miocene	N_1^1		

Table 2 Characteristics of seismic reflection units in deepwater canyons

Seismic reflection units	External morphology	Internal reflection texture	Amplitude	Continuity	Termination
BES	Concave	N/A	High	High	Erosive
TD	Lenticular	Parallel	High	High	Onlap
LMP	Filling	Oblique/S-type	Low	Middle	Downlap
MTD	Irregular	Disorder	Variable	Low	Erosive
OL-OD	Sheet	Parallel/subparallel	Low-middle	Middle-high	Erosive
ILD	Hummocky	Disorder/subparallel	Middle-high	Middle-high	Downlap
CMD	Sheet	Subparallel	Low-middle	Low-middle	Erosive
DD	Sheet drape	Parallel	High	High	Erosive
CLZ	Penicillate	Wave	Variable	Low	Erosive
L/SSD	Sheet/hummocky	Parallel	High	High	Onlap

yons, indicating that their axes are steep and dominant in erosion. The draping depositions are found at the top of canyons, which may be relevant to the near position away from their sources. In the cross-section B (Fig. 5b), the axis of a single canyon widens and its flanks become gradually gentle, showing U-type. The BES migrates conspicuously to the northeastern direction in a great amount of movement. The internal formation within LMP dips apparently towards the east. There exist a lot of draping depositions at the top of these canyons, which suggests that there are rich sediments coming here. In the cross-section C (Fig. 5c), by comparison to the cross-section B, the amount of lateral migration gradually decreased with time in BES and LMP and eventually transform from the lateral migration into the vertical overlay pattern. According to the ODP1148 borehole data, this transformation occurs in Pliocene (about 5 Ma). The single canyon is mainly in vertical aggradational filling each other. The draping depositions develop very well at the top and there are irregular-shaped MTD outside of canyons, including slide, slump, and debris-flow deposits.

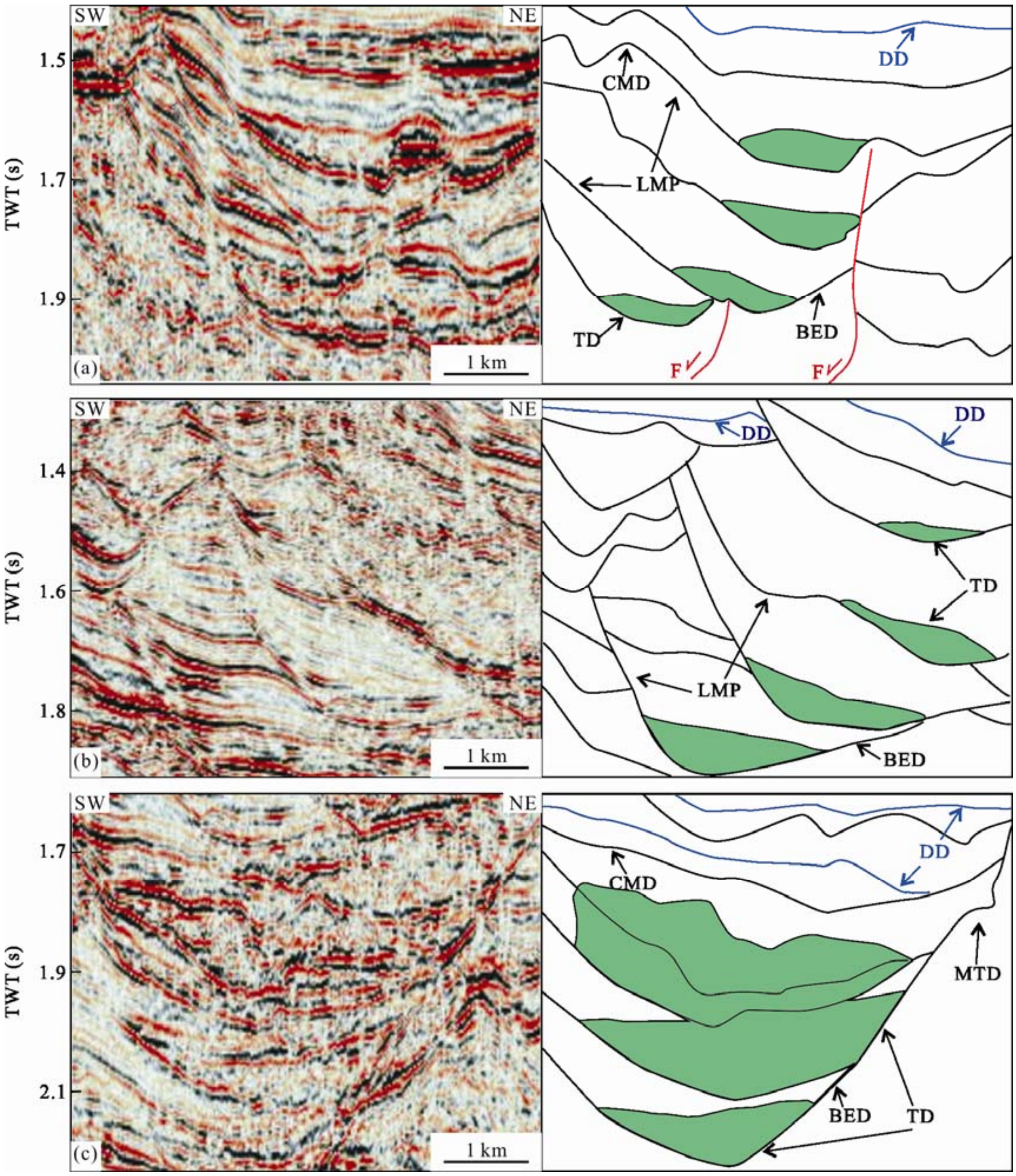

Figure 5. Seismic reflection units of C9 in cross-section profiles (the location is shown in Fig. 2).

EVOLUTION PROCESSES OF DEEPWATER CANYONS

Based on their stratigraphic ages and morphological characteristics, the evolution processes of the studied canyons are divided into three stages: (1) scouring-filling stage (Middle Miocene), (2) lateral migration stage (Late Miocene), and (3) vertical overlay stage (Pliocene–Quaternary) (Fig. 6). However, the main factors controlling the development of the studied canyons are different at the three stages and they are explained in detail as follows.

At the scouring-filling stage (Middle Miocene, T4–T3) (Fig. 6a), the canyons in the cross-section show V-type, suggesting their main scouring-fillings effects, and the episode forming a single canyon is vague, indicating that the rapid accumulation and filling of sediments within canyons may occur after forming incised valleys. During the Middle Miocene, there exist deep fractures to dip gently towards the south extending tens to hundreds of kilometers in the study area, and some of which dissect the erosion surface of canyons, revealing that the deep fractures are the inner generative forces inducing the studied canyons. Therefore, in this stage, the studied canyons are mainly due to the eroding and scouring of turbidity currents down the slope and being influenced by tectonic activities.

At the lateral migration stage (Late Miocene, T3–T2) (Fig. 6b), the episode forming a single canyon is obvious, and the relative sea-level fluctuation in a cycle makes the canyons form inherited erosion and sedimentary filling cycles. The axes of canyons show prominent features of lateral migration towards the northeast. It is asymmetric at the two flanks of canyons, and the southwestern flank developing lots of LMP is relatively gentle, while the northeastern one is very steep because of its erosion or weak sedimentations. During the period of low-stand level, there are a large number of clastic materials to supply by turbidity currents down the slope; then, turbidity currents become gradually strong and even exceed sustainable bottom currents along the slope (parallel to the slope strike) in the end, occurring BES and TD. In comparison, during the period of high-stand level,

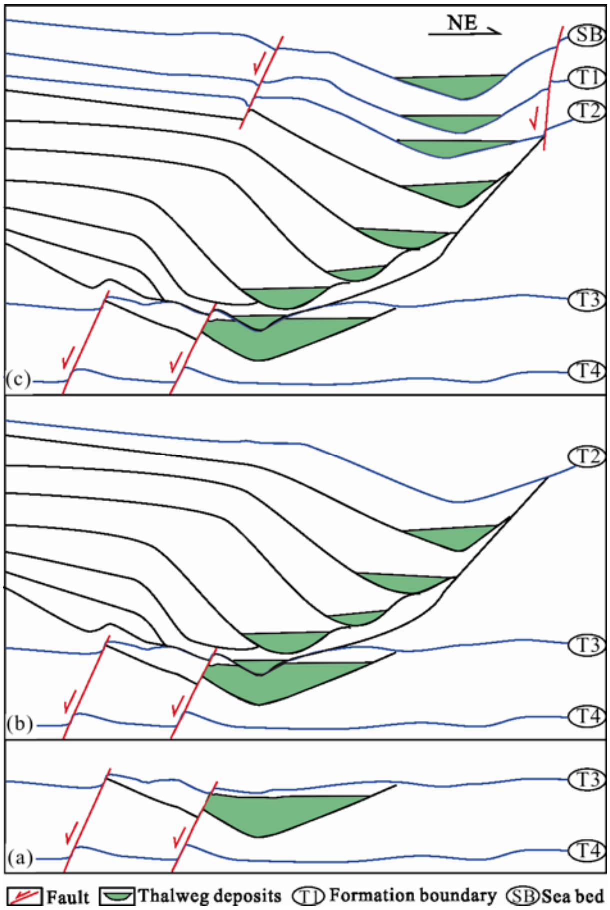

Figure 6. Evolution models of the studied canyons. (a) Middle Miocene; (b) Late Miocene; (c) Pliocene–Quaternary.

turbidity currents gradually weaken and eventually disappear, while bottom currents play a main role, developing LMP and being preserved very well. Luan et al. (2010) pointed out that sand waves on the northern shelf of the SCS were to a great extent in equilibrium with oceanographic bottom current condition. The canyon formation in this stage is thus attributed to the double roles of turbidity and bottom currents.

At the vertical overlay stage (Pliocene–Quaternary, T2–SB) (Fig. 6c), most of canyons are active to date, showing V-type open submarine canyons, and the single canyon vertically overlays each other. In the Early Pliocene, there are normal faults dipping to the south in the study area, especially the most notable at the bottom of C11–C17 in the east (Fig. 3). This may indicate that, after the swelling of strata in the Dongsha Islands, the SCS basin closes further since the Pliocene and the bottom current becomes weak. Thus, in this stage, the studied canyons are mainly due to the eroding and sedimentary filling by turbidity currents.

From west to east in the study area, the WD becomes gradually deeper in the location originating canyons, and their evolution processes are slightly different each other (Fig. 3). The C1–C10 in the west develop a little earlier in the Miocene, including the scouring-filling stage, the lateral migration stage, and the vertical overlay stage. On the other hand, the C11–C17 in the east developed later in the Late Miocene, mainly including the lateral migration stage. During the Pliocene, C12–C17 were almost inactive and there exist transtensional normal faults dipping toward the south at the top of canyons instead. In the Late Quaternary, there were other new incising valleys to be found on the topmost of faults, which are open and have not yet been completely filled so far. However, the C11 shows the transitional characteristics of the two different kinds of evolution processes in the east and in the west.

GENETIC MECHANISM OF DEEPWATER CANYONS

Tectonic Activity and Deepwater Canyons

In the Cenozoic era, BS is located in the structural transform zone of rifts, where tectonic deformation and magmatic activity are very strong, which has evolved three periods, including the early rifting period from Late Cretaceous to Early Eocene, the late rifting period from Middle Eocene to Early Oligocene, and the post-rifting period from Middle Oligocene to nowadays. It is clearly different from the typical double-layer rifting basin in passive continental margins, experiencing only the rifting and post-rifting period. In the center of BS, the Cenozoic strata thickness is more than 10 km (Pang et al., 2007, 2004; Huang et al., 2005).

In the 2D high-resolution multi-channel seismic reflection profile in the NW-SE strike through the study area (Fig. 7), there are deep faults mainly dipping to the south in the NW-SE strike in the northern part of BS, most of which continue until the Late Miocene (T3), and a few faults go upward through the Pliocene reflection surface (T2) and even broke the seafloor. Since the Pliocene, in the northern slope of BS, there occur two sets of dextral shear faults being active later in the NE-SW or near E-W and the NNE-SSW strike (Figs. 1 and 3). The formation of these faults may be caused by the moving of the Philippine Sea plate to the west, which is called Dongsha movement, and this movement leads to block-faulting fluctuation and tectonic inversion in the eastern part of PRMB, whose influences decrease from east to west (Sun et al., 2008; Yu et al., 2007).

During the Pliocene, canyons C12–C17 are not

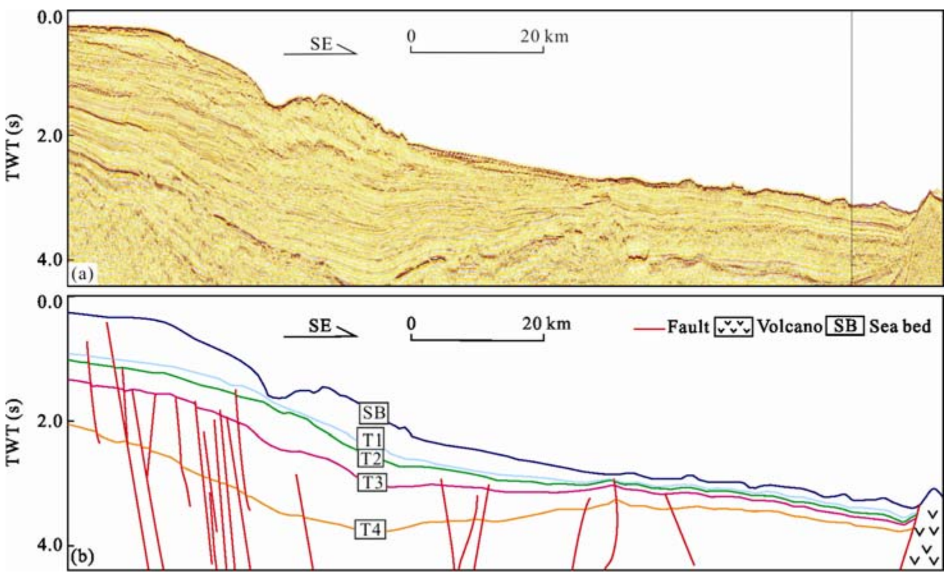

Figure 7. Characteristics of strata and fractures in BS. (a) Original seismic profile (the measuring line is shown in Fig. 1); (b) the drawing line.

active temporarily, but there is a normal fault dipping to the south at the bottom of each canyon. In the Late Quaternary, it develops correspondingly another new scouring-filling valley at the topmost of each fault. This suggests that the faults are the initial driving force triggering the studied canyons (Figs. 3, 5a, and 7). In our opinion, the faulting makes strata become soft, which is conducive to being eroded by flows, or producing a number of debris and small pieces of materials, which is transported directly into canyons by flows. In the lower or near the end of C4–C16, their axes change suddenly from south to southeast, as well as C17 is in the NW-SE direction, which is closely relevant to a series of NWW-SEE transtensional faults produced by the Dongsha movement. Also, the studied canyons in near N-S direction are unanimous with the NNE-SSW normal fault dipping to the south in Pliocene. Since the Pliocene, the C1–C10 present vertical overlay and filling in the western part of the study area, while the eastern C12–C17 stop acting temporarily and there occur transtensional faults dipping to the south instead. In other words, the results are concordant with the strength of tectonic inversion decreasing from east to west caused by the Dongsha movement, and the transformation of filling patterns from lateral migration to vertical overlay (about 5 Ma) is also compatible with the stable tectonic environment after Dongsha swelling.

Double Mechanisms of Turbidity and Bottom Currents

The formation and evolution of deepwater canyons are related to a series of factors, such as subsea topography, sediment substrate, relative sea-level fluctuation, tectonic activity, the discharge and nature of flows, whether connecting with the land river or not, and so on. Among them, the flows related above are mainly sediment gravity flow—turbidity currents and bottom currents. Most of deepwater canyons in passive continental margins are caused by turbidity currents, while there are a few ones referring to bottom currents, e.g., Goitaca in Brazil (Viana, 2002), Gabon in West Africa (Rasmussen, 1994), and Rockal in the North Atlantic (Howe, 1996).

In general, deepwater turbidity canyon-channels evolve in four stages, including the bottom erosion, the lateral migration changing thalweg morphologies, the vertical overlay and filling caused by the autocyclical turbidity currents, and the semi-pelagic draping stage (Tinterria et al., 2003; Peakall et al., 2000; Kuenen and Migliorini, 1950), which is accompanied by the collapsing of canyon-channel sidewalls or the formation of MTD during their evolution periods. When the slope angle is larger than 0.3° in the upper slope where canyon-channels exist, canyon-channels are straight and show V-type in their cross-section, which is formed by the incising and eroding of turbidity currents; when the slope angle is less than 0.3° in the middle and lower slope, canyon-channels extend in a meander and show U-type in their cross-sections, which is due to the sedimentation and filling of turbidity currents (Wynn et al., 2007). The slope angle in the study area is about 1–3° and the studied canyons extend straightly (Fig. 2), which is the same as turbidity canyons. In addition, the obvious BES, the coarse-grained TD, and the approximately 95% fine-grained components in the sedimentary are all evidences of turbidity currents.

However, in the cross-section profile (Fig. 5b), the two flanks of canyons are asymmetric. The southwestern flank is gentle showing significant lateral migration and progradation, while the northeastern one is steep suggesting erosion or weak sedimentation. In our opinion, this lateral migration may be due to bottom currents flowing from the NE to the SW in the intermediate-upper deepwater layer (about 350–1 350 m WD) (Fig. 8). The southwestern flank lies in the upstream of flows at a low rate, with the corresponding low bed shear stress and a high sedimentary rate, showing a gentle slope. In comparison, the northeastern one is in the downstream of flows at a high rate, the corresponding high bed shear stress and a low sedimentary rate and even erosion occurring, as a result of a steep slope. Shao et al. (2007) elaborate a propagating southwestward sedimentary drift to the southeast of the Dongsha Islands, which follows the direction of the bottom currents from the NE to the SW on the northern continental slope of SCS. This work is in conformity with the view of Shao et al.

(2007). The circulation system in SCS is very complex. This study indicates that there is little change in the WD of study area since the Miocene, and the direction of ocean currents is also the same as these days (Shao et al., 2007; Li Q Y et al., 2006; Li B H et al., 2005; Wang et al., 2000), which can be used as evidence of restoring paleogeographic environments.

The characteristics of the studied canyons are

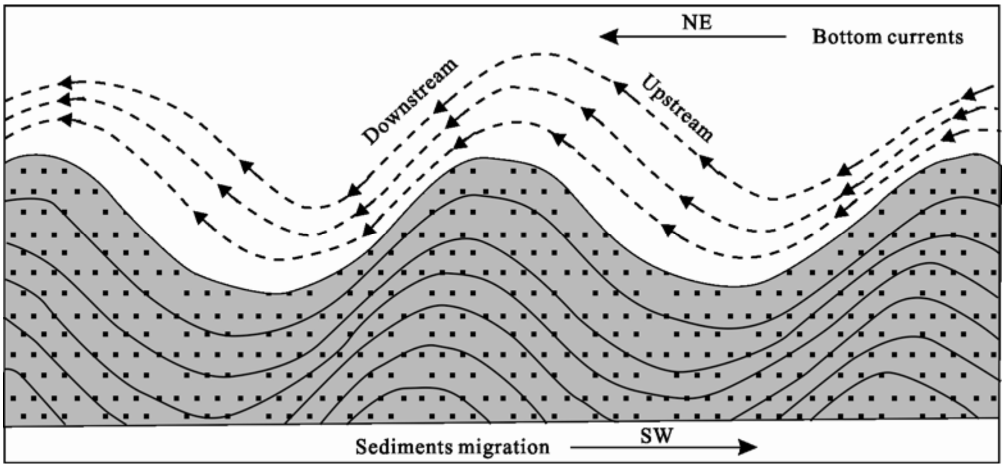

Figure 8. Sediments migration model of bottom currents.

different from the turbidity canyons that are purely caused by turbidity currents. The two flanks of straight turbidity canyons are usually symmetry, but the two flanks of meandering ones are asymmetry because of the Coriolis effect. If the studied canyons were affected by the Coriolis effect, which should have make turbidity currents deflect to the right side (the SW direction) in the northern hemisphere, as a result, the southwestern flank should be steep because of eroding by turbidity currents and the northeastern flank should be gentle. In fact, the characteristics of the studied canyons are contrary with the hypothesis above. Thus, the lateral migration is not caused by Coriolis effect. Moreover, the $\delta^{18}O$ values of planktons and benthoses in the ODP1148 drilling and the carbonate dissolution events have shown that the study area is influenced by bottom currents since the Miocene, and the current direction is in agreement with the intermediate-upper deep water (350–1 350 m) (Shao et al., 2007; Li Q Y et al., 2006; Li B H et al., 2005). The Luzon Strait is a main passageway for the water mass exchanging between the SCS and the Pacific Ocean. Most physical oceanographers agree that during the winter the water flows from the Pacific Ocean inpour into the SCS through the Luzon Strait, while there are many different view points about the flow direction during the summer (Yang et al., 2010; Qu, 2002). Bao et al. (2009) and Fang et al. (2009) suggested outward flows from the Pacific Ocean to the SCS north of Dongsha Islands.

In a word, the genetic mechanisms of the studied canyons are very complicated, which is caused by the double effects of turbidity and bottom currents and influenced by the faults at the bottom as the initial driving forces. Among them, the BES and the coarse-grained TD are the result of the erosion, sedimentation and filling by turbidity currents, but the LMP in the southeastern flank is due to bottom currents.

CONCLUSIONS

In the northern slope of BS, there occur deepwater canyons since the Middle Miocene, originating below the shelf break, extending in the near N-S direction, which are approximately oblique with the slope. However, these canyons are not deeply eroded into the continental shelf, indicating that they have not reached to their mature evolution stages. In the downstream or near the end of the canyons, their strike directions change abruptly from the south to the southeast and even some of them turn to the near W-E. All studied canyons show similar sedimentary characteristics and evolution processes in seismic profiles. There is BES at the bottom, which is covered by TD, then LMP occurring above, MTD or CMD developing in the flanks of canyons and mantling DD at the top. The upper segments of these canyons show scouring/eroding and V-type, while the lower ones exhibit sedimentation/filling and U-type, which are similar to the typical deepwater turbidity canyons in the world.

According to the stratigraphical ages and geometrical features of these canyons, their formation and evolution processes are divided into three stages, which are Middle Miocene scouring-filling, Late Miocene lateral migration, and Pliocene–Quaternary vertical overlay. A autocyclic progressive process of eroding and filling by turbidity currents results in the scouring-filling and vertical overlay; bottom currents are responsible for the remarkable asymmetry between the two flanks of canyons, and the southwestern flanks are gentle showing significant lateral migration and progradation, while the northeastern ones are steep suggesting erosion or weak sedimentation. This may be due to the bottom currents flowing from the NE to the SW in the intermediate-upper deep water layer (about 350–1 350 m WD) since the Middle Miocene. In addition, these canyons have different evolution processes from east to west in the study area, and they change abruptly from the south to the southeast in the downstream or near the end, which may be related to a series of transtensional faults produced by the Dongsha Movement in Pliocene. In a word, the BES and coarse-grained TD are due to turbidity currents, but the LMP are the witnesses of bottom currents. Therefore, the studied canyons are caused by the double effects of turbidity and bottom currents under the control of faults as inherent dynamic forces.

REFERENCES CITED

Bao, X. W., Ju, X., Wu, D. X., 2009. Characteristics of Water Exchange across 120°E Secrion in the Luzon Strait. *Periodical of Ocean University of China*, 39(1): 1–6 (in Chinese with English Abstract)

Bouma, A. H., Stelting, C. E., Coleman, J. M., 1984. Mississippi Fan: Internal Structure and Depositional Processes. *Geo-Marine Letters*, 3: 147–153

Damuth, J. E., Flood, R. D., 1985. Amazon Fan, Atlantic Ocean. In: Bouma, A. H., Normark, W. R., Barnes, N. E., eds., Submarine Fans and Related Turbidite Systems. Springer Verlag, New York. 97–106

Dong, D. D., Wu, S. G., Zhang, G. C., et al., 2008. Rifting Process and Formation Mechanisms of Syn-Rift Stage Prolongation in the Deepwater Basin, Northern South China Sea. *Chinese Science Bulletin*, 53(23): 3715–3725

Droz, L., Rigaut, F., Cochonat, P., et al., 1996. Morphology and Recent Evolution of the Zaire Turbidity Systems (Gulf of Guinea). *Geological Society of American Bulletin*, 108(3): 253–269

Emmel, F. J., Curray, J. R., 1985. Bengal Fan, Indian Ocean. In: Bouma, A. H., Normark, W. R., Barnes, N. E., eds., Submarine Fans and Related Turbidite Systems. Springer Verlag, New York. 107–112

Fang, G. H., Wang, Y. G., Wei, Z. X., et al., 2009. Interocean Circulation and Heat and Freshwater Budgets of the South China Sea Based on a Numerical Model. *Dynamics of Atmospheres and Oceans*, 47: 55–72

Heinio, P., Davies, R. J., 2007. Knickpoint Migration in Submarine Channels in Response to Fold Growth, Western Niger Delta. *Marine and Petroleum Geology*, 24: 434–449

Howe, J. A., 1996. Turbidite and Contourite Sediment Waves in the Northern Rockall Trough, North Atlantic Ocean. *Sedimentology*, 43(2): 219–234, doi:10.1046/j.1365-3091.1996.d01-1.x

Huang, C. J., Zhou, D., Sun, Z., et al., 2005. Deep Crustal Structure of Baiyun Sag, Northern South China Sea Revealed from Deep Seismic Reflection Profile. *Chinese Science Bulletin*, 50(11): 1131–1138, doi:10.1360/04wd0207

Kolla, V., Coumes, F., 1987. Morphology, Internal Structure, Seismic Stratigraphy, and Sedimentation of Indus Fan. *AAPG Bulletin*, 71: 650–677

Kolla, V., Posamentier, H. W., Wood, L. J., 2007. Deep-Water and Fluvial Sinuous Channels—Characteristics, Similarities and Dissimilarities, and Modes of Formation. *Marine and Petroleum Geology*, 24: 388–405

Kuenen, P. H., Migliorini, C. I., 1950. Turbidity Currents as a Cause of Graded Bedding. *Journal of Geology*, 58(2): 97–127

Li, B. H., Jian, Z. M., Li, Q. Y., et al., 2005. Paleoceanography of the South China Sea since the Middle Miocene: Evidence from Planktonic Foraminifera. *Marine Micropaleontology*, 54: 49–62

Li, Q. Y., Wang, P. X., Zhao, Q. H., et al., 2006. A 33 Ma

Lithostratigraphic Record of Tectonic and Paleoceanographic Evolution of the South China Sea. *Marine Geology*, 230: 217–235

Luan, X. W., Peng, X. C., Wang, Y. M., et al., 2010. Activity and Formation of Sand Waves on Northern South China Sea Shelf. *Journal of Earth Science*, 21(1): 55–70, doi:10.1007/s12583-010-0005-4

Pang, X., Chen, C. M., Shao, L., et al., 2007. Baiyun Movement: A Great Tectonic Event on the Oligocene–Miocene Boundary in the Northern South China Sea and Its Implications. *Geological Review*, 53(2): 145–152 (in Chinese with English Abstract)

Pang, X., Yang, S. K., Zhu, M., et al., 2004. Deep-Water Fan Systems and Petroleum Resources on the Northern Slope of the South China Sea. *Acta Geologica Sinica*, 78(3): 626–631

Peakall, J., Mccaffrey, B., Kneller, B., 2000. Perspectives: A Process Model for the Evolution, Morphology and Architecture of Sinuous Submarine Channels. *Journal of Sedimentary Research*, 70(3): 434–448, doi:10.1306/D4268C20-2B26-11D7-8648000102C1865D

Pirmez, C., Beaubouef, R. T., Friedmann, S. J., et al., 2000. Equilibrium Profile and Base Level in Submarine Channels: Examples from Late Pleistocene Systems and Implications for the Architecture of Deepwater Reservoirs. In: Weimer, P., Slatt, R. M., Coleman, J., et al., eds., Deepwater Reservoirs of the World. CSSEPM Foundation 20th Annual Research Conference (CD-Rom, GCSSEPM), Huston. 782–805

Pirmez, C., Imran, J., 2003. Reconstruction of Turbidity Currents in Amazon Channel. *Marine and Petroleum Geology*, 20: 823–849

Prather, B. E., Booth, J. R., Steffens, G. S., et al., 1998. Classification, Lithologic Calibration and Stratigraphic Succession of Seismic Facies of Intraslope Basins, Deep-Water Gulf of Mexico. *AAPG Bulletin*, 82: 701–728

Qu, T. D., 2002. Evidence for Water Exchange between the South China Sea and the Pacific Ocean through the Luzon Strait. *Acta Oceanologica Sinica*, 21(2): 175–185

Rasmussen, E. S., 1994. The Relationship between Submarine Canyon Fill and Sea-Level Change: An Example from Middle Miocene Offshore Gabon, West Africa. *Sedimentary Geology*, 90(1–2): 61–75

Shao, L., Li, X. J., Geng, J. H., et al., 2007. Deep Water Bottom Current Deposition in the Northern South China Sea. *Science in China* (*Series D*), 50(7): 1060–1066

Sun, L. T., Zhou, D., Chen, C. M., et al., 2008. Fault Structure and Evolution of Baiyun Sag in Pearl River Mouth Basin. *Journal of Tropical Oceanography*, 27(2): 25–31 (in Chinese)

Tinterria, R., Dragob, M., Consonni, A., et al., 2003. Modelling Subaqueous Bipartite Sediment Gravity Flows on the Basis of Outcrop Constraints: First Results. *Marine and Petroleum Geology*, 20: 911–933

Viana, A. R., 2002. Seismic Expression of Shallow to Deep-Water Contourites along the South-Eastern Brazilian Margin. *Marine Geophysical Researches*, 22: 509–521

Wang, P. X., Prell, W. L., Blum, P., et al., 2000. Proceedings of the Ocean Drilling Program, Initial Reports South China Sea. *College Station TX*, 184: 18–20

Weimer, P., Slatt, R. M., 2007. Introduction to the Petroleum Geology of Deepwater Settings. *AAPG Bulletin*, 57(8): 149–277

Wynn, R. B., Cronin, B. T., Peakall, J., 2007. Sinuous Deep-Water Channels: Genesis, Geometry and Architecture. *Marine and Petroleum Geology*, 24: 341–387

Xie, X. N., Muller, R. D., Li, S. T., et al., 2006. Origin of Anomalous Subsidence along the Northern South China Sea Margin and Its Relationship to Dynamic Topography. *Marine and Petroleum Geology*, 23: 745–765

Yang, Q. X., Tian, J. W., Zhao, W., 2010. Observation of Luzon Strait Transport in Summer 2007. *Deep-Sea Research I*, 57: 670–676

Yu, H. S., Chang, E. T. Y., 2009. Links among Slope Morphology, Canyon Types and Tectonics on Passive and Active Margins in the Northernmost South China Sea. *Journal of Earth Science*, 20(1): 77–84, doi:10.1007/s12583-009-0008-1

Yu, S. M., Mei, L. F., Shi, H. S., et al., 2007. Relationship between Faults and Hydrocarbon Accumulation in Panyu Low Massif and North Slope of Baiyun Sag, Pearl River Mouth Basin. *Petroleum Exploration and Development*, 34(5): 562–579 (in Chinese)

Zhao, Q. H., 2005. Late Cainozoic Ostracod Faunas and Paleoenvironmental Changes at ODP Site 1148, South China Sea. *Marine Micropaleontology*, 54(1–2): 27–47

Zhu, M. Z., Graham, S., Pang, X., et al., 2010. Characteristics of Migrating Submarine Canyons from the Middle Miocene to Present: Implications for Paleoceanographic Circulation, Northern South China Sea. *Marine and Petroleum Geology*, 27: 307–319